JOURNAL OF SOLID STATE CHEMISTRY **124,** 238–243 (1996)
ARTICLE NO. 0232

Sodium Intercalation into $(PbS)_{1.18}(TiS_2)_2$ Misfit Layer Compound

P. Lavela, J. Morales, and J. L. Tirado

Laboratorio de Química Inorgánica, Facultad de Ciencias, Universidad de Córdoba, E-14004, Córdoba, Spain

Received February 13, 1996; accepted April 1, 1996

The misfit layer sulfide of composition $(PbS)_{1.18}(TiS_2)_2$ has been studied as a host material for the intercalation of sodium. The discharge curve profile using propylene carbonate (PC) as the solvent of electrolyte showed that the intercalation process is complex with the appearance of an extended plateau which suggests the formation of a multiphase region. In fact, an intermediate phase of sodium content 0.2 mol per formula unit, with basal spacing of 29.9 Å, which exceeds by 12.4 Å the repeating unit $PbS–TiS_2–TiS_2$, has been observed. This result is interpreted on the basis of solvent cointercalation. PC molecules are located at the interlayer region defined at the interface $TiS_2–TiS_2$. The increase in the sodium content promotes the release of PC molecules out of the layers. The interlayer expansion of the new phase formed is similar to that observed upon intercalation with sodium naftalide and is consistent with the location of sodium ions in the interstitial sites defined by two consecutive sulfur slabs. Under room conditions this phase absorbs water. The final expansion of ca. 6 Å is consistent with a bilayer hydration process.

INTRODUCTION

In the last few years, a family of compounds with nonstoichiometric composition $(MS)_{1+x}(TS_2)_2$ (M = Pb, Sn, Bi, Ln; T = Ti, Nb, Ta) has been synthesized. Until now, X-ray single crystal structures have been determined for $(PbS)_{1.12}(NbS_2)_2$ (1) and $(PbS)_{1.18}(TiS_2)_2$ (2). These systems consist of two successive TS_2 slabs alternating with an MS double layer. For a more detailed description of the structures and transport properties of these compounds, the reader is referred to an excellent review by Wiegers and Meerschaut (3). Since typical van der Waals gaps separate two adjacent TS_2 slabs, one subject of particular interest in these systems is the study of their intercalation properties that may affect their electronic properties.

Recently, lithium was intercalated into some of these systems (4–7), either chemically or electrochemically. The results obtained from the electrochemical intercalation of lithium into $(PbS)_{1.18}(TiS_2)_2$ showed that this compound can form distinct $Li_x(PbS)_{1.18}(TiS_2)_2$ phases (7). In this work, we extend this investigation to the study of the intercalation of sodium and we present further details of the characterization of the intercalate phases observed.

EXPERIMENTAL

$(PbS)_{1.18}(TiS_2)_2$ was prepared by direct synthesis from powdered elements as described elsewhere (2, 5). Powder X-ray diffraction patterns were obtained on a Siemens D500 diffractometer using Cu$K\alpha$ radiation and a graphite monochromator. Thermogravimetric analysis (TGA) was carried out in a Cahn 2000 electrobalance.

Chemical sodium intercalation was done by stirring the solid in 0.125 M sodium naftalide solution in tetrahydrofuran (THF) in a dry box (M. Braun) under an Ar atmosphere. Electrochemical measurements were performed in $Na/NaClO_4$–PC/sulfide cells assembled and discharged under argon atmosphere. Intermediate products were prepared to observe structural changes due to sodium insertion into the host lattice by halting the electrochemical experiments at different depths of discharge. Galvanostat Intermittent Titration Technique (GITT) was used to obtain the quasi-equilibrium curve. For this purpose, the cell was discharged in steps $x = 0.05$ at 20 $\mu A \cdot cm^{-2}$ with a relaxation condition of 0.5 $mV \cdot h^{-1}$. Step potential electrochemical spectroscopy (SPES) measurements were used for evaluating the reversibility of the system. An initial relaxation of the cells was allowed until a ratio $\Delta V/\Delta t \leq 2$ $mV \cdot h^{-1}$ was reached. Spectra were recorded with constant voltage steps of 10 $mV \cdot h^{-1}$. All the electrochemical measurements were monitored by a multichannel microprocessor control system McPile.

RESULTS AND DISCUSSION

The ternary misfit compound of nominal composition $(PbS)_{1.18}(TiS_2)_2$ was obtained as microcrystalline powder with a metallic luster. The semiquantitative atomic percentages of Pb (12.5), Ti (23.0), and S (64.6) determined by energy dispersive X-ray analysis in the platelike particles agree fairly well with the above mentioned stoichiometry.

The structure, determined from single crystal X-ray diffraction data (2), consists of two consecutive blocks of TiS_2

0022-4596/96 $18.00

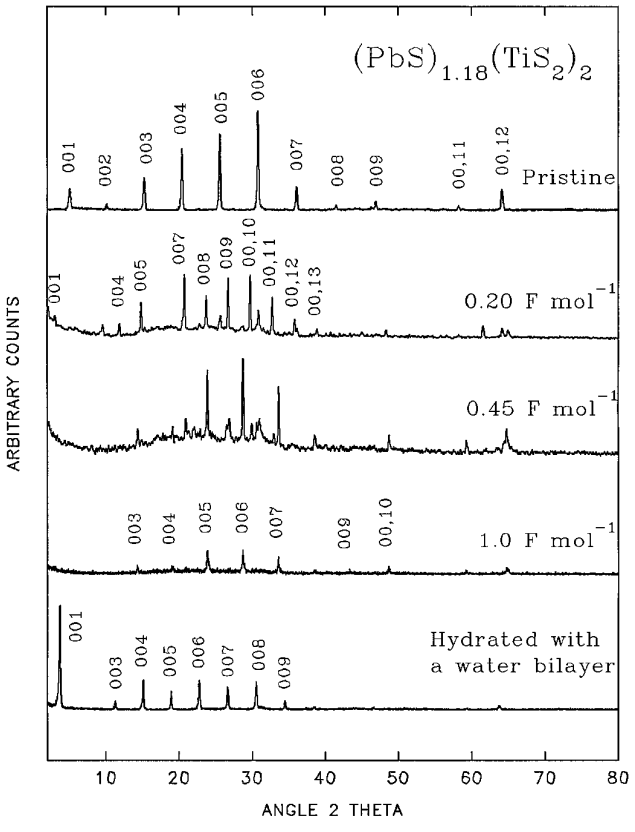

FIG. 1. X-ray powder diffraction data of pristine, electrochemically sodium intercalated products at different depths of discharge and bilayer hydrated phase of $(PbS)_{1.18}(TiS_2)_2$.

separated by PbS double layers which are stacked along the *c* axis. The powder XRD pattern of the pristine sulfide is shown in Fig. 1. Due to the preferred orientation of the particles associated with the use of a powder diffractometer, only a group of 00*l* reflections can be clearly seen. The periodic length obtained, 17.45(1) Å, is in good agreement with the *c* dimension determined in Ref. (2).

The electron diffraction pattern of pristine $(PbS)_{1.18}(TiS_2)_2$ obtained by allowing the electron beam to incide perpendicularly to the layers was characteristic of TiS_2 and PbS sublattices intergrowth, as reported elsewhere (8). Also, the reciprocal cells had unequal a^* axes, which is an indirect evidence that the two subsystems are mutually incommensurate.

A typical galvanostatic intermittent titration curve for $Na_x(PbS)_{1.18}(TiS_2)_2$ is shown in Fig. 2. Data were obtained at room temperature. Two plateaus are observed at about 2.20 and 1.55 V. These constant voltage regions are located in the composition ranges $0.18 < x < 0.3$ and $x > 0.6$, respectively, which means thermodynamically that there is a multiphase system. Between these plateaus, the voltage decreased sharply with the increase of concentration. This behavior resembles that of the Na–TiS_2 system for which different constant plateaus corresponding to two phase regions have been reported over the composition range $0 < x \leq 1$ (9, 10). Nevertheless, the cell potential and the nature of the phenomenon are quite different as will be described below.

Qualitatively, the discharge curve of the $(PbS)_{1.18}TiS_2$ phase, whose structure consists of alternately stacked PbS double layers and TiS_2 sandwiches (3), shows significant differences with respect to that of the $(PbS)_{1.18}(TiS_2)_2$ phase (Fig. 2). The sharp voltage decrease down 1.0 V in the first discharge region just above a sodium content of 0.1 per formula is indicative of a much lower cell discharge capacity. This implies that sodium intercalation is inhibited in this phase, probably because of the stronger interlayer interactions that affect PbS and TiS_2 slabs, instead of the presence of a true van der Waals gap between two consecutive TiS_2 slabs, which are present in the bilayer compound $(PbS)_{1.18}(TiS_2)_2$. The PbS substructure consists of a double layer of NaCl type with Pb and S lying in parallel planes but with the metal atoms protruding from the sulfur plane. In fact, a significant covalent interaction of *M* atoms with sulfur atoms of TS_2 has been proposed to explain the stability of these compounds (11). This feature is probably responsible for the limited intercalation properties of $(PbS)_{1.18}TiS_2$ that only intercalates lithium to a small extent (5). However, the larger size of Na ions apparently inhibits its intercalation.

To throw light on the structural changes in the host caused by the intercalation process and to correlate them with the electrochemical behavior, several X-ray powder diffraction patterns were recorded over the $0 < x < 1$ composition range. Figure 1 shows the most relevant patterns for describing the system with accuracy. When sodium is intercalated up to $x = 0.2$ new considerably smaller peaks appear alongside the reflections of the original

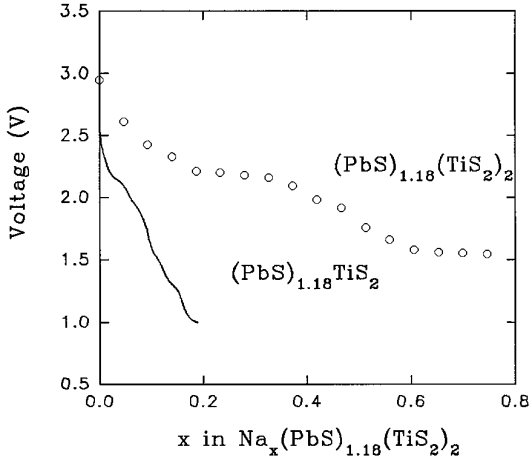

FIG. 2. Open circuit voltage curve for $(PbS)_{1.18}(TiS_2)_2$ and discharge curve, recorded at 100 $\mu A \cdot cm^{-2}$, for $(PbS)_{1.18}TiS_2$.

phase. The new peaks make a set of multiple order reflections with a basal spacing of 29.9 Å. This value exceeds the basal spacing of the original compound, 17.45 Å, which defines the repeating $PbS–TiS_2–TiS_2$ unit by about 12.4 Å. Thus, a model in which sodium atoms occupy every $TiS_2–TiS_2$ interlayer, either in octahedral or trigonal prismatic coordination, must be ruled out. In fact, the maximal expansion reported for the intercalation of Na into TiS_2 is ca. 1.3 Å (12) and corresponds to a phase composition of $Na_{0.5}TiS_2$, a stage I compound with sodium ions located in trigonal prismatic sites.

Further sodiation ($x = 0.45$) results in the appearance of a new set of multiple-order reflections with a basal spacing of 18.6 Å. The phase with a large basal spacing is preserved, whereas the diffraction peaks associated with the parent compound disappear. Finally, for a sodium content of ca. 1 F/mole, a continuous loss of long range ordering is made evident from the broadening and the decrease in the intensity of the 00*l* reflections. This can be intrepeted as a consequence of the structural amorphization. The only distinguishable phase is that with a basal spacing of 18.6 Å.

In this context, it is worth noting that chemical intercalation with sodium naftalide also yields a phase with a basal spacing of 18.7 Å. Unfortunately, the degree of sodium intercalation could not be accurately determined owing to the difficulty in eliminating traces of the intercalating reagent. However, the XRD pattern of this sample was similar to that recorded for a degree of electrochemical intercalation of ca. 1 F/mole. Thus, it seems reasonable to identify the 18.7 Å phase as a stage I compound in which the sodium ions occupy the middle positions of the sulfur interlayers.

We interpret the high basal spacing phase as a consequence of solvent cointercalation. Several tests support this conclusion. First, different reports have demonstrated that propylene carbonate (PC) may penetrate into the structure of layered host together with alkali ions during the electrochemical intercalation. Thus, PC intercalation has been observed in Li/TiS_2 (13) and Li/β-ZrNCl (M = Li, Na, K) cells (14). It causes a large expansion of the interlayer spacing close to 12 Å which corresponds to the formation of a double layer of propylene carbonate coordinated to the alkali ions placed at the center of the interlayer (15). This value is quite similar to that obtained from the intercalate with sodium content $x = 0.2$. A more detailed structural characterization of this intermediate was obtained by using one-dimensional electron density maps along the *c* axis. One-dimensional Patterson diagrams were used to evaluate interatomic distances along [001] in the structure of the pristine sulfide and the intercalated products. These diagrams were constructed from the intergral intensity of 12 00*l* reflections (I_{10}), corrected from absorption, Lorentz, and polarization effects, by applying the following Fourier transform:

$$P(u) = (1/c) \sum_1 F_1^2 \cos(2\pi l u). \quad [1]$$

From the u values in which the maxima of the Patterson function were detected, the z coordinates of the different atoms were calculated and a set of phased structure factors F_1 was generated. These were then used to calculate values of I_{1c} which were compared with the experimental values by computing the R Bragg factor:

$$R_B = \sum |I_{1o} - I_{1c}| / \sum I_{1o}. \quad [2]$$

After optimization of the z values, the one-dimensional electron density function was then computed along the z axis of the structure, according to the following expression:

$$\varphi(Z) = (1/c) \sum F_1 \cos(2\pi l z). \quad [3]$$

The projection of the electron density for both the original and the 29.9 Å phases is shown in Fig. 3. Since there is a direct relationship between the number of electrons of the atoms and the X-ray scattering, the heavier the atoms the higher the intensity of the signal in the diagram. In this sense, the diagram corresponding to the pristine compound (Fig. 3a) shows a group of peaks with different intensities. The higher ones are those originated by the presence of the PbS slabs as the lead atoms are the dominant X-ray scatterers. The adjacent triplets which are placed at the center of the plot are due to the presence of two adjacent TiS_2 slabs.

The projection of the electron density for the high basal spacing phase with sodium stoichiometry equivalent to $x = 0.2$ is shown in Fig. 3b. The main difference between this plot and that of the electron density of the host is the appearance of new peaks between the TiS_2 slabs while the region defined at the interface $PbS–TiS_2$ remains unaltered. The increase in the electron density in the $TiS_2–TiS_2$ interlayer can be attributable to the Na ions co-intercalated with PC molecules which are responsible for the large expansion of the interlayer spacing.

Indirect evidence for this model was obtained from thermogravimetric data recorded under nitrogen atmosphere. Two electrochemical cells were prepared. One was discharged up to $x = 0.2$ while the other was kept in an open circuit for the same period of time used in the first cell. Afterward, pellets were carefully dried with a blotting paper in order to remove the residual solvent without detaching any particle from the surface. The TG plots are shown in Fig. 4. It is clearly observed that the weight loss of the nondischarged sample is negligible with respect to that of the sodium intercalated compound. The small weight loss observed for the undischarged sample can be

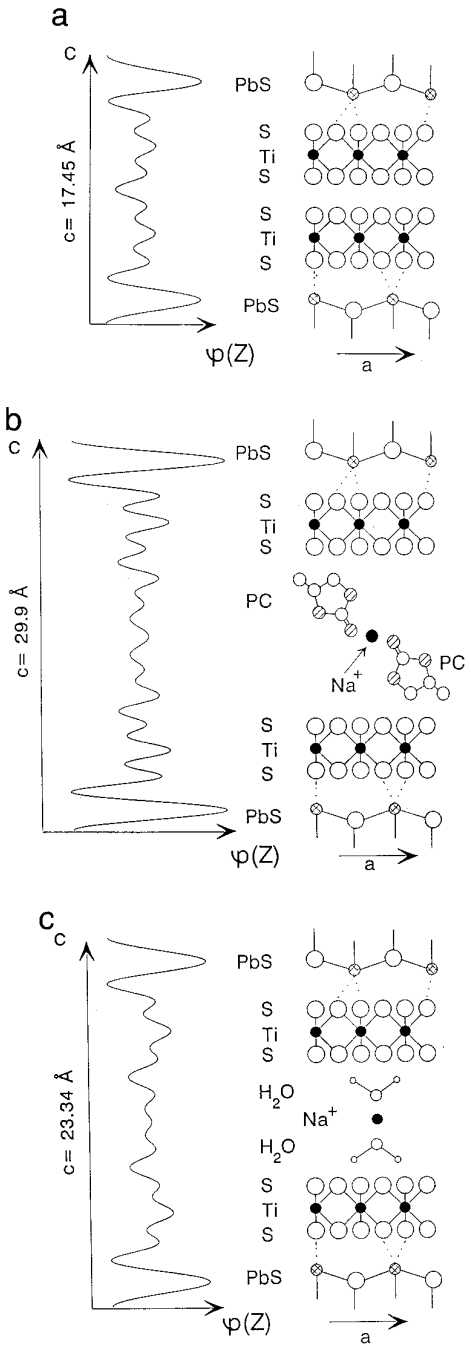

FIG. 3. One-dimensional electron distribution maps along the *c* axis obtained for (a) pristine compound, (b) $Na_{0.2}(PC)_{0.75}(PbS)_{1.18}(TiS_2)_2$, and (c) $Na(PbS)_{1.18}(TiS_2)_2$ under room conditions.

associated with PC adsorbed on the particle surface. For the discharged pellet, the weight loss extends over 120–320°C and is basically consistent with the release of PC molecules more strongly bound to the host. Thus, we explain this weight by means of the release of the co-intercalated solvent. From a quantitative evaluation of the TG data, the composition of the complex was determined to be $Na_{0.2}(PC)_{0.75}(PbS)_{1.18}(TiS_2)_2$.

The former results support the conclusion that the PC molecules are likely able to penetrate into the structure simultaneously to the sodium insertion and to expand the TiS_2–TiS_2 interlayer up to 12.4 Å. The driving force for co-intercalation is due to dipole–cation interactions. The phenomenon takes place if the interaction between the polar solvent molecule and the cation in the interlayer space is strong enough to compensate the energy required for expanding the interlayer space. The solvation energy is given by the equation (15)

$$\Delta G = -\frac{N(z)^2}{8\pi\varepsilon_0\gamma}(1 - 1/\varepsilon), \qquad [4]$$

where N is the Avogadro's number, z is the ionic charge, and ε and ε_0 are the dielectric constants of solvent and vacuum, respectively. In this context, discharge properties were investigated using γ-butyrolactone (BA) as solvent of electrolyte. This solvent has a smaller dielectric constant (39.5) than PC (64.4) and thus a smaller solvation energy. The XRD pattern of the discharge products up to a sodium content of $x = 0.2$ did not show any evidence of the occurrence of a high basal spacing phase, and the new set of diffraction lines observed was comparable to that for 18.6 Å phase. Thus, co-intercalation of BA was not observed because of the smaller dielectric constant of this solvent.

We think that the solvent intercalation probably occurs only into the external crust of the particles for several reasons. First, we could not obtain a pure high basal spacing

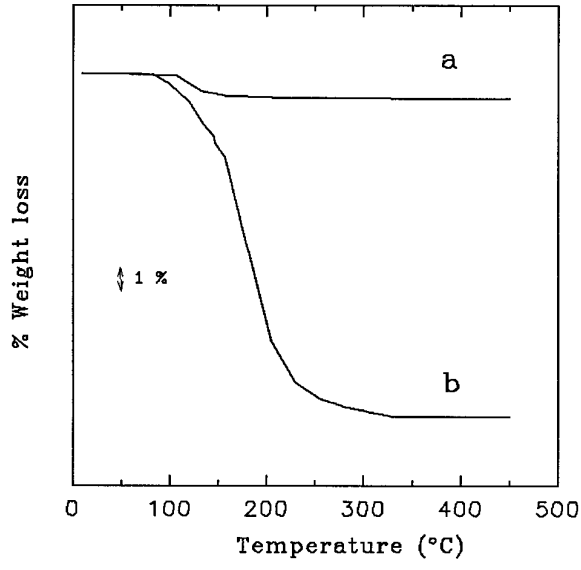

FIG. 4. Thermogravimetric curve of the (a) undischarged and (b) discharged ($x = 0.2$) cathodic material.

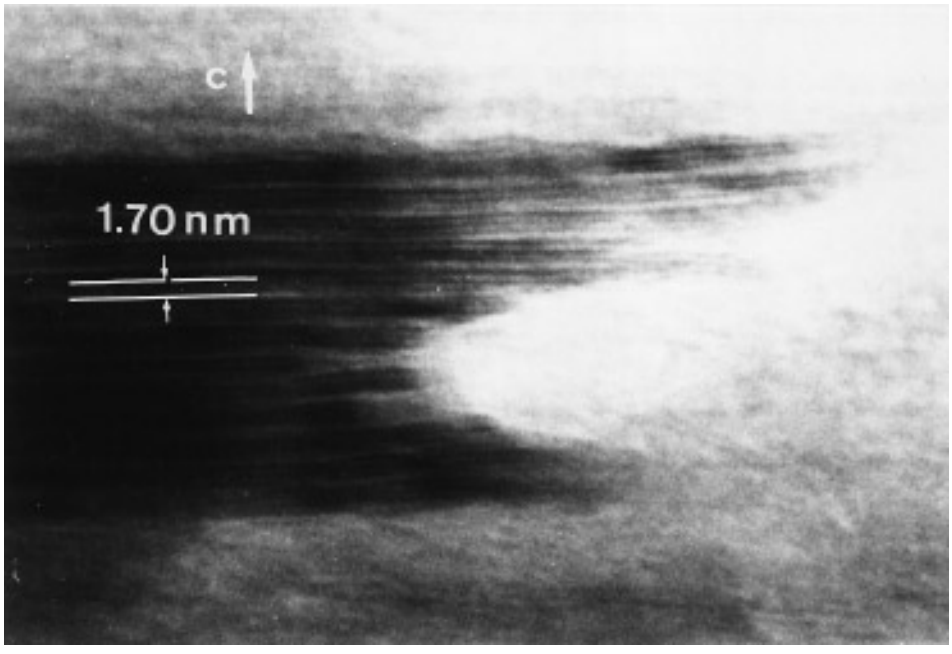

FIG. 5. Bright-field TEM image of $Na_{0.2}(PC)_{0.75}(PbS)_{1.18}(TiS_2)_2$ with incident beam normal to [001].

phase. Either pristine or unsolvated intercalated phases were always present at the same time. This fact can be explained in terms of a heterogeneous composition of the particles. Evidence of this behavior is shown by the electron microscopy images, Fig. 5. Careful observation of the right side of the $Na_{0.2}(PbS)_{1.18}(PC)_{0.75}(TiS_2)_2$ image reveals a significant splitting of the lattice fringes near the edge of the particles. Once the solvent molecules penetrate into the host, their displacement in the interlayer space toward the inner core of the particles is prevented because of the molecule size. Thus, cointercalation occurs at the early stage and the plateau defined in the interval is consistent with the coexistence of sodium co-intercalated with solvent and pristine material in agreement with the biphasic character of the process. The XRD patterns corresponding to the intermediate samples in the composition range $0.35 < x < 0.6$ (Fig. 1) showed a progressive disappearance of the high basal spacing phase. The remaining phase has a periodic length of 18.6 Å which is ascribed to the sodium ion intercalation. It seems that, as the amount of sodium intercalated increases, the high basal spacing phase collapses releasing the solvated PC molecules out of the layers. This behavior has been also observed by Ohashi *et al.* (14) in the Li-tetrahydrofurane (THF) system and has been explained by assuming that as the lithium ion content increases, the electrostatic interactions between these cations and the negatively charged layers may overcome the solvatation energy of the Li-THF system. This gives rise to the removal of the solvent out the lattice and the maintenance of the alkali ions in the interlayer space. Thus, the conclusion reported by some authors (13, 14) concerning the irreversibility of the co-intercalation process, i.e. that co-intercalated PC cannot be removed electrochemically, is controversial.

Step potential electrochemical spectroscopy (SPES) technique was used to study the reversibility of the intercalation process. Figure 6 shows the current versus voltage plot. In these plots, the plateaus appear as peaks and the intensity of the signal is related to charge passing through the cell. The lower curve corresponds to the intercalation reaction and the upper curve to the reverse process. It is noteworthy that the profiles of both processes are completely different. The discharge curve shows an intense signal ($I = 0.045$ mA) which defines the first plateau observed in the galvanostatic curve. In contrast, the reverse curve does not show any significant peak at a similar potential. These results suggest that the solvent molecules cannot be reintercalated once they are extruded from the interlayer space during the reduction process.

Recently, we have also reported the formation of a high basal spacing phase for the $Li/(PbS)_{1.18}(TiS_2)_2$ system at low discharge depths (7). Based on the interlayer expansion and on the fact that co-intercalation phenomenon is usually described as irreversible in the literature (13), we interpreted this intercalate in terms of lithium ordering by assuming that every third interlayer region TiS_2–TiS_2 is occupied by lithium ions. Apparently, this assumption is not consistent with the results discussed above. In light of these results, we have calculated the one-dimensional electron density projection on the *c* axis, Fig. 7, and it

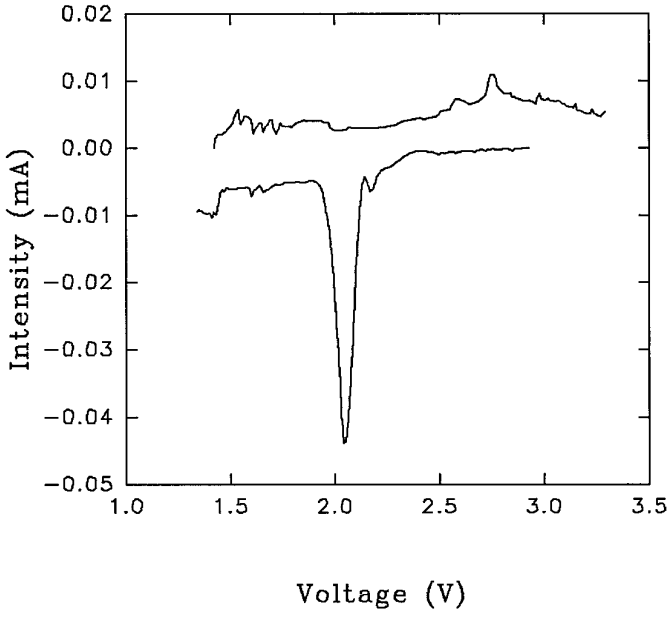

FIG. 6. Step potential electrochemical curves of the Na/$NaClO_4$(PC)/$(PbS)_{1.18}(TiS_2)_2$ cell.

basically resembles that shown in Fig. 3b. Thus, the expansion of the interlayer distance is also consistent with the location of the PC molecules in the interlayer region of the host compound.

One relevant feature worth commenting on is the structural change observed when the alkali metal intercalates are exposed to the air. The X-ray pattern of a sample of limiting composition $Na(PbS)_{1.18}(TiS_2)_2$, basal spacing 18.6 Å, supports the idea of the formation of hydrated phases which reach a final basal spacing of 23.34(7) Å; see Fig. 1. The expansion observed, ca. 6 Å, is roughly twice the van de Waals diameter of a water molecule and can be ascribed to a bilayer hydration process of the intercalated cations. The one-dimensional electron density map along the *c* axis is shown in Fig. 3c. The peaks which appear between the contribution of TiS_2 layers are consistent with the presence of two layers of water molecules in the interlayer region. The hydration process probably takes place via a mechanism similar to that found for the hydration of $Li_2(PbS)_{1.18}(TiS_2)_2$ (16). First, a hydrated monolayer, basal spacing 20.68(5) Å, is formed that slowly evolves to a bilayer hydrate stage.

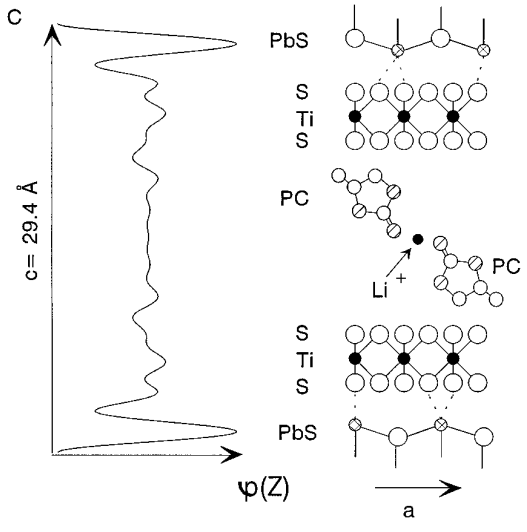

FIG. 7. One-dimensional electron distribution map along the *c* axis obtained for the high basal spacing phase detected upon electrochemical lithium intercalation in $(PbS)_{1.18}(TiS_2)_2$.

In contrast, the high basal spacing phase is highly unstable under similar experimental conditions. The Na^+ ions are readily extruded and the material recovers the structure of the pristine compound. Therefore, the energy required to initiate the separation of the TiS_2 layer must be significant, so under simple aerobic conditions it is possible to relieve the crystal strain, thereby reducing the overall crystal energy by extrusion of guest species.

ACKNOWLEDGMENT

We express our gratitude toward the CICYT (Contract MAT 93-1204).

REFERENCES

1. A. Meerschaut, L. Guemas, C. Auriel, and J. Rouxel, *Eur. J. Solid State Inorg. Chem.* **27,** 557 (1990).
2. A. Meerschaut, C. Auriel, and J. Rouxel, *J. Alloys Comp.* **183,** 129 (1992).
3. G. A. Wiegers and A. Meerschaut, *in* "Sandwiched Incommensurate Layered Compounds" (A. Meerschaut, Ed.). Trans. Tech. Pub., Zurich, 1992.
4. C. Auriel, A. Meerschaut, P. Deniard, and J. Rouxel, *C. R. Acad. Sci. Paris Ser. II* **313,**1255 (1991).
5. L. Hernan, P. Lavela, J. Morales, J. Pattanayak, and J. L. Tirado, *Mater. Res. Bull.* **26,** 1211 (1991).
6. L. Hernan, J. Morales, J. Pattanayak, and J. L. Tirado, *J. Solid State Chem.* **100,** 262 (1992).
7. C. Barriga, P. Lavela, J. Morales, J. Pattanayak, and J. L. Tirado, *Chem. Mater.* **4(5),** 1021 (1992).
8. S. Kuypers, J. Van Landuyt, and S. Amelinckx, *J. Solid State Chem.* **86,** 212 (1990).
9. D. A. Winn, J. M. Shemilt, and B. C. H. Steele, *Mater. Res. Bull.* **11,** 559 (1976).
10. P. Molinie, L. Trichet, J. Rouxel, C. Berthier, Y. Chebre, and P. Segransan, *J. Phys. Chem. Solids* **45(1),** 105 (1984).
11. A. R. H. F. Ettema, G. A. Wiegers, C. Haas, and T. S. Turner, *Surf. Sci.* **269/270,** 1161 (1992).
12. H. H. Whangbo, J. Rouxel, and L. Trichet, *Inorg. Chem.* **24,** 1824 (1985).
13. J. R. Dahn, M. A. Py, and R. R. Hearing, *Can. J. Phys.* **60,** 307 (1982).
14. M. Ohashi, K. Uyeoka, S. Yamanaka, and M. Hattori, *Bull. Chem. Soc. Jpn.* **64,** 2814 (1991).
15. T. Yamamoto, S. Kikkawa, and M. Koizumi, *J. Electrochem. Soc.* **131(6),** 1343 (1984).
16. P. Lavela, J. Morales, and J. L. Tirado, *Chem. Mater.* **4,** 2 (1992).